Neurochem Res (2011) 36:2063–2074
DOI 10.1007/s11064-011-0530-2

ORIGINAL PAPER

p53- and Bax-Mediated Apoptosis in Injured Rat Spinal Cord

Ramaprasada Rao Kotipatruni · Venkata Ramesh Dasari · Krishna Kumar Veeravalli · Dzung H. Dinh · Daniel Fassett · Jasti S. Rao

Accepted: 7 June 2011 / Published online: 7 July 2011

Abstract Spinal cord injury (SCI) induces a series of endogenous biochemical changes that lead to secondary degeneration, including apoptosis. p53-mediated mitochondrial apoptosis is likely to be an important mechanism of cell death in spinal cord injury. However, the signaling cascades that are activated before DNA fragmentation have not yet been determined. DNA damage-induced, p53-activated neuronal cell death has already been identified in several neurodegenerative diseases. To determine DNA damage-induced, p53-mediated apoptosis in spinal cord injury, we performed RT-PCR microarray and analyzed 84 DNA damaging and apoptotic genes. Genes involved in DNA damage and apoptosis were upregulated whereas anti-apoptotic genes were downregulated in injured spinal cords. Western blot analysis showed the upregulation of DNA damage-inducing protein such as ATM, cell cycle checkpoint kinases, 8-hydroxy-2′-deoxyguanosine (8-OHdG), BRCA2 and H2AX in injured spinal cord tissues. Detection of phospho-H2AX in the nucleus and release of 8-OHdG in cytosol were demonstrated by immunohistochemistry. Expression of p53 was observed in the neurons, oligodendrocytes and astrocytes after spinal cord injury. Upregulation of phospho-p53, Bax and downregulation of Bcl2 were detected after spinal cord injury. Sub-cellular distribution of Bax and cytochrome c indicated mitochondrial-mediated apoptosis taking place after spinal cord injury. In addition, we carried out immunohistochemical analysis to confirm Bax translocation into the mitochondria and activated p53 at Ser^{392}. Expression of APAF1, caspase 9 and caspase 3 activities confirmed the intrinsic apoptotic pathway after SCI. Activated p53 and Bax mitochondrial translocation were detected in injured spinal neurons. Taken together, the in vitro data strengthened the in vivo observations of DNA damage-induced p53-mediated mitochondrial apoptosis in the injured spinal cord.

Keywords Apoptosis · Bax · DNA damage · Microarrays · p53 · Spinal cord injury

Abbreviations

ALS	Amyotrophic lateral sclerosis
ANOVA	Analysis of variance
APAF1	Apoptotic protease activating factor 1
ATM	Ataxia telangiectasia mutated
ATR	Ataxia telangiectasia and Rad3 related
BRCA2	Breast cancer 2, early onset
BSA	Bovine serum albumin
CHAPS	3-[(3-Cholamidopropyl)dimethylammonio] propanesulfonic acid
CHK2	Checkpoint homolog (*S. pombe*)
CNS	Central nervous system
DAB	Diaminobenzidine
DAPI	4′,6-Diamidino-2-phenylindole dihydrochloride

Ramaprasada Rao Kotipatruni and Venkata Ramesh Dasari contributed equally.

Electronic supplementary material The online version of this article (doi:10.1007/s11064-011-0530-2) contains supplementary material, which is available to authorized users.

R. R. Kotipatruni · V. R. Dasari · K. K. Veeravalli · J. S. Rao (✉)
Department of Cancer Biology and Pharmacology, University of Illinois College of Medicine at Peoria, One Illini Drive, Peoria, IL 61656, USA
e-mail: jsrao@uic.edu

D. H. Dinh · D. Fassett · J. S. Rao
Department of Neurosurgery, University of Illinois College of Medicine at Peoria, Peoria, IL, USA

DNA	Deoxyribonucleic acid
DSB	Double-strand breaks
DTT	Dithiothreitol
EDTA	Ethylenediaminetetraacetic acid
ELISA	Enzyme-linked immunosorbent assay
FBS	Fetal bovine serum
FITC	Fluorescein isothiocyanate
GFAP	Glial fibrillary acidic protein
H2AX	Histone H2A.X
HEPES	4-(2-hydroxyethyl)-1-piperazineethanesulfonic acid
HRP	Horseradish peroxidase
hUCB	Human umbilical cord blood derived stem cells
Olig2	Oligodendrocyte transcription factor 2
PAGE	Poly acrylamide gel electrophoresis
PBS	Phosphate buffered saline
RT-PCR	Reverse Transcription based Polymerase chain reaction
PMSF	Phenyl methane sulfonyl fluoride
SCI	Spinal cord injury
SDS	Sodium dodecyl sulfate
SSB	Single-strand breaks
STP	Staurosporine
TAE	Tris-acetate-EDTA
TUNEL	Terminal deoxynucleotidyl transferase dUTP nick end labeling

Introduction

Neuronal apoptosis is mediated by the mitochondrial-mediated pathway in a majority of neurodegenerative diseases. For instance, in cerebral ischemia, neurodegeneration is mediated by p53 activation and Bax translocation [1, 2]. Spinal cord injury (SCI) results in the initial physical disruption of structures in the spinal cord (primary injury) and in the generation of secondary events that collectively injure the otherwise intact neighboring tissue. Secondary pathogenesis of spinal cord injury is the most devastating event caused by neuronal cell apoptosis. Our recent study demonstrated the upregulation of mitochondrial apoptotic genes such as Bad, Bid, Bid3, Bcl10, Bcl2a1, Bik and Bak1 in the injured rat spinal cords [3]. SCI induced by trauma compresses and shears neuronal and glial cell types and their processes in the immediate vicinity of the impact. As a consequence, cells spill their intracellular contents into the extracellular matrix. This pathophysiological occurrence initiates a cascade of biochemical changes that results in necrotic and apoptotic cell death [4].

Although DNA damage may ensue from excitotoxicity and other stresses possibly as a result of increased production of reactive oxygen species, DNA damage is a common activator of neuronal injury [5]. These cellular stresses are linked to the activation of numerous downstream signaling pathways such as the cyclin-dependent and stress-activated kinases, DNA-dependent protein kinase, ATM and p53. Once activated in neurons, p53 appears to have a major impact on mitochondrial integrity, which revolves around members of the Bcl-2 family [5]. p53 influences the expression and/or activity of the pro-apoptotic proteins, Bax and APAF1. Several of these proteins affect mitochondrial membrane permeability (e.g., Bax) or the activation of apoptotic mediators downstream of the mitochondria (e.g., APAF1). p53 promotes Bax translocation from the cytosol to the outer membrane of the mitochondria [6]. The relationship between p53 expression and neuronal cell death has been evaluated in numerous models of injury and disease [7]. Recently transcription factor p53 was identified in degenerating the spinal cord of ALS patients [8]. p53 promotes apoptosis by modulating the expression of select target genes. Numerous pro-apoptotic genes are susceptible to regulation by p53, including Bax. [9]. Bax was reported to be a cytosolic protein in healthy living cells and upon induction of apoptosis, it translocates to the mitochondria [10–12]. This translocation process is rapid and occurs at an early stage of apoptosis [12]. It has been reported that the intracellular movement of Bax to the mitochondria depolarizes the mitochondria and induces the release of cytochrome c, which causes the adaptor APAF1 to activate caspases 9 and 3 and ultimately cellular demise [13, 14]. Finally, no studies have been reported to ascertain the role of Bax in the secondary pathogenesis of spinal cord injury-mediated neuronal cell death. Thus, our overall goal was to determine the molecular mechanism(s) by which SCI elicits its apoptotic effects on neuronal cells adjacent to the injured spinal cord.

The present study is designed to demonstrate p53 activation and Bax-mediated mitochondrial apoptosis in injured spinal cords of rat in vivo and spinal neurons in vitro. To date, no information exists regarding the DNA damage linked to neuronal apoptosis after spinal cord injury. Therefore, this study was designed to investigate the level of DNA damage and expression of genes involved in apoptosis after SCI.

Experimental Procedures

Preparation of Primary Cell Cultures of Spinal Neurons

Primary cultures of spinal neurons were prepared from embryonic 18-day Sprague–Dawley rats as previously described [15]. Spinal cords were obtained from Brain Bits (Springfield, IL) and triturated gently (8–10 times) in cold Hibernate-E medium plus 1× B27-supplement (Invitrogen,

Carlsbad, CA) and 1% penicillin-streptomycin (Invitrogen). Once in suspension, the cells were diluted in 1 mL of the same medium and the number of viable cells was determined by Trypan blue exclusion. Cells were plated at a density of 0.25×10^6 cells/μL on poly-D-lysine-coated (50 μg/mL) plates in neurobasal medium. Cultures were maintained at 37°C in a humidified 5% CO_2 atmosphere, and all experiments were performed after 12–15 days in culture. Cultures were fed every 3 days with fresh medium. All experiments were performed in neurobasal medium containing 2% antioxidant-free B27-supplement. Under these culture conditions, only neuronal cells survive. These cultures were comprised of approximately 90–95% neuronal cells as confirmed by immunocytochemical staining performed according to the manufacturer's instructions with anti-NeuN (Abcam, Cambridge, MA) or anti-neurofilament 200kDa (Chemicon, Temecula, CA) antibodies.

Spinal Cord Injury of Rat

Moderate spinal cord injury was induced using the weight drop device (NYU Impactor) as reported previously [16, 17]. Briefly, adult male rats (Lewis; 250–300 g) were anesthetized with ketamine (100 mg/kg; ip) and xylazine (5 mg/kg; ip) (Med-Vet International, Mettawa, IL). A laminectomy was performed at the T9–T11 level exposing the cord beneath without disrupting the dura, and the exposed dorsal surface of the cord at T10 was subjected to a weight drop impact using a 10 g rod (2.5 mm in diameter) dropped at a height of 12.5 mm. The animals were sacrificed at different time points (1, 3, 7, 14 and 21 days). The Institutional Animal Care and Use Committee of the University Of Illinois College Of Medicine at Peoria approved all surgical interventions and post-operative animal care.

Determination of Caspase 9 Activity

A quantitative enzymatic activity assay was performed using Caspase 9 Assay kit (R&D Systems, Minneapolis, MN). Tissue lysates at different time points were incubated at 37°C in buffer supplemented with substrate LEHD-7-amino-4-trifluoromethyl coumarin (AFC) (25 μM) for caspase 9. Protease activity of caspase 9 was monitored using a substrate with an optimized bifunctional cell lysis/activity buffer. Samples were assayed at 499 nm absorbance on the BioRad plate reader. Specific inhibition of caspase 9 was achieved by the addition of caspase inhibitor AC-LEHD-CHO.

Determination of Caspase 3 Activity

Caspase 3 activity of tissue lysates at different time points was measured using a caspase 3 assay kit (Sigma, St. Louis, MO). Injured and sham operated spinal cord tissues were homogenized in 1× lysis buffer (50 mM HEPES, pH 7.4, 5 mM CHAPS, 5 mM DTT) and the homogenates were then centrifuged at 20,000×*g* for 15 min at 4°C in a microcentrifuge. We analyzed the supernatants for caspase 3 activity levels using the 96-well plate microassay method. In a final volume of 100 μL, supernatants (50 μg protein) of each test sample were incubated for 30 min at room temperature in the working solution containing Ac-DEVD-AMC, a synthetic caspase 3 substrate. Absorbance was read at 405 nm on an ELISA plate reader for a period of 30 min. We used Ac-DEVD-CHO inhibitor for the inhibitor studies. Caspase 3 activity was calculated using a *p*-nitro aniline calibration curve. The data were plotted as A_{405} versus time for each sample and activity was calculated as pmol/min.

Staurosporine-Induced Apoptosis in Cultured Rat Spinal Neurons

After 12–15 DIV (days in vitro), primary spinal neurons (E18) were exposed to 2 μM staurosporine for 4 h at 37°C to induce apoptosis. After the neurons had been exposed to staurosporine for the required time, the cells were detached from the plates by gentle scraping and were centrifuged at 500×*g* for 3 min. The supernatant was removed, and the pellet was resuspended in PBS and centrifuged again at 500×*g* for 3 min to wash the cells. The supernatant was discarded, and the cell pellet resuspended in 1 mL of propidium iodide (50 μg/mL) solution. The samples were analyzed using a flow cytometer (BD FACS Calibur, BD Biosciences, Franklin Lakes, NJ).

Immunoblot Analysis

For immunoblot analysis, rats were euthanized, and 1–4 mm lengths of spinal cord from the injury site were rapidly removed, weighed, and frozen at −80°C until necessary for further experimentation. The tissues were resuspended in 0.2 mL of homogenization buffer (pH 7.4, 250 mM sucrose, 10 mM HEPES, 10 mM Tris–HCl, 10 mM KCl, 1% NP-40, 1 mM NaF, 1 mM Na_3VO_4, 1 mM EDTA, 1 mM DTT, 0.5 mM PMSF plus the following protease inhibitors: 1 μg/mL pepstatin, 10 μg/mL leupeptin and 10 μg/mL aprotinin), homogenized in a Dounce homogenizer, and processed as described previously [18]. For Western blot analysis, the following antibodies were used: rabbit anti-phospho-p53 (Abcam), rabbit anti-Bax, mouse anti-Bcl-2, and mouse anti-GAPDH (Santa Cruz Biotechnology, Santa Cruz, CA). In a similar fashion, cell lysates from untreated and treated spinal neurons were processed. Experiments were performed in triplicate to ensure reproducibility. Values for injured, treated and control samples ($n \geq 3$ each group) were

compared using one-way ANOVA test. A p value of <0.05 was considered significant.

Isolation of Genomic DNA and Agarose Gel Electrophoresis

DNA laddering is one of the hallmark events used to confirm apoptosis. Internucleosomal DNA fragmentation in the spinal cord tissue of control and spinal cord tissue adjacent to the site of injury (caudal) in injured (1, 3, 7, 14 and 21 days post-SCI) rats was determined using the TACS DNA Laddering Kit (R&D Systems, Minneapolis, MN). Briefly, DNA extraction from tissue samples was performed as per the manufacturer's instructions. Tissue was minced into small pieces and then frozen in liquid nitrogen. Frozen tissue was powdered and lysed with the buffers provided in the kit. DNA present in the lysed tissue was extracted using the extraction solutions and followed by addition of sodium acetate. DNA pellets were obtained by adding 2-propanol to the extracted solution followed by centrifugation at $12{,}000\times g$ for 10 min. DNA pellets were washed with 70% ethanol, dried and resuspended in DNase-free water. Samples (2 μg/lane) were loaded onto 1.6% agarose gels containing ethidium bromide, electrophoresed in $1\times$ TAE buffer and photographed on an UV transilluminator.

PCR Super Array analysis

We used the RT2 Profiler Rat Apoptosis PCR Array (Catalog No. APRN-012, SA Biosciences, Frederick, MD). Spinal cords of sham control and 3 weeks SCI injured rats were removed as per the study design. Approximately 1 cm of the segments, including the injury site, were collected and homogenized. Total RNAs of respective tissue segments were isolated and approximately 1 μg of total RNA from each sample was synthesized into cDNA following manufacturer's instructions using the iScript^{TM}cDNA Synthesis Kit (Bio-Rad Laboratories, Hercules, CA). Real-time PCR was carried out under the following conditions: one cycle of 95°C for 10 min, and 40 cycles of 95°C for 15 s and 60°C for 1 min. Changes in gene expression were illustrated as a fold increase/decrease. The cut-off induction for determining expression was $+2.0$ or -2.0 fold changes. Genes that fit the above criteria were considered to be upregulated or downregulated. Nine rats were used for each group (sham control and 3 weeks SCI) and the RNA extracted from three individual rats was pooled and used. We performed these experiments in duplicate.

Immunohistochemistry

Animals were sacrificed at different time points (1, 3, 7, 14 and 21 days after SCI) for studies on apoptosis under in vivo conditions. Rats were anesthetized with ketamine/xylazine and intracardially perfused with 4% paraformaldehyde in 0.1 M phosphate buffer (pH 7.4). The spinal cords were removed and fixed for 2 h. Serial sections (5 μm) were made from the spinal cord and stained with H&E and Luxol fast blue for assessment of tissue morphology and to determine the injury epicenter. Sections (1 section every 200 μm) obtained from 1 to 4 mm of tissue caudal to the epicenter were used for immunohistochemical analysis of activated apoptotic proteins. After staining with primary antibodies (1:100 dilution), the sections were washed three times in PBS (10 min/wash) and incubated in goat anti-mouse or anti-rabbit HRP-conjugated secondary antibodies (1:200 dilution). For immunofluorescence studies, the sections were washed three times in PBS (10 min/wash) and incubated in Alexa Fluor 594 conjugated anti-mouse secondary antibody or Alexa Fluor 488 conjugated anti-rabbit secondary antibody (all at 1:200 dilutions) for 1 h at room temperature. Sections were then washed three times in PBS (10 min/wash), counterstained with DAPI, cover slipped using fluorescent mounting medium (Dako, Carpentaria, CA) and observed under a confocal microscope (Olympus Fluoview, Olympus, Melville, NY). Negative controls (without primary antibody or using isotype-specific IgG) were maintained for all the samples. Sections in which polymerase was omitted were used as the negative control for TUNEL assay. A neuropathologist, who was blinded to the treatment groups and study, evaluated the sections.

Evaluation of Cell Death by TUNEL Assay

To determine the number of apoptotic cells in the tissue sections, paraffin-embedded tissue sections were deparaffinized and rehydrated. Samples were then incubated in TUNEL reaction mixture in a humidified atmosphere for 1 h at 37°C in the dark and washed with PBS. 4′, 6-diamidino-2-phenylindole (DAPI) staining mounting solution was used for nuclear counterstaining. Samples were imaged with an Olympus fluorescence microscope. The apoptotic index was defined as follows: apoptotic index (%) = 100 × (apoptotic cells/total cells).

Sub-Cellular Fractionation of Mitochondria and Cytosolic Fractions

Spinal neurons were harvested, washed once with cold PBS, and resuspended in ice-cold buffer A of Mitochondria isolation kit (Sigma). Cells were then Dounce homogenized and unbroken cells and nuclei were removed by centrifugation at $500\times g$ for 5 min at 4°C. The supernatants were further centrifuged at $7{,}700\times g$ for 10 min at 4°C to obtain the crude mitochondrial fraction. The supernatants resulting from the

above step were subjected to a high-speed centrifugation at 100,000×*g* for 1 h at 4°C to obtain the cytosolic fraction. The crude mitochondrial pellet was resuspended in cold buffer A and layered on the top of a 2.5 M sucrose-percoll gradient and centrifuged at 46,000×*g* for 45 min at 4°C to separate the pure mitochondrial fraction. The mitochondria were collected and washed twice with buffer A at 7,700×*g* for 10 min at 4°C and lysed in the presence of cold buffer A plus 1% Chaps for 30 min at 4°C. The lysates were then centrifuged at 15,000×*g* for 10 min at 4°C to remove insoluble debris. Protein concentration of both mitochondrial and cytosolic lysates was determined using the Bradford dye-binding protein assay (Bio-Rad).

Comet Assay

DNA damage was assessed using the alkaline single-cell gel electrophoresis (SCGE) "comet assay" method. The comet assay has been shown to be a sensitive and reliable measure of DNA strand breaks associated with incomplete excision repair sites and alkali-labile sites. In the present study, we used the OxiSelect Comet Assay Kit (Cell Biolabs Inc, San Diego, CA). Spinal cord tissue was processed by re-suspension in PBS (10,000 cells/mL). 50 μL of the cell suspension was then mixed with 500 μL of 0.5% low melting point agarose at 37°C and 75 μL of the cell/agarose mixture was transferred onto glass slides. Slides were immersed in pre-chilled lysis buffer (2.5 M NaCl, 100 mM EDTA, 10 mM Tris, pH 10.0, 1% Triton X-100, and 10% Me_2SO) for 1 h, followed by equilibration in Tris borate-EDTA (TBE) buffer for 30 min. Slides were electrophoresed in TBE at 1.5 volt/cm for 5 min and stained with Vistra Green. Images were visualized under a fluorescence microscope and captured with a CCD camera. Nuclei with damaged DNA have the appearance of a comet with a bright head and a tail, whereas nuclei with undamaged DNA appear round with no tail. The olive tail moment is one of the parameters that are commonly measured with the comet assay. It represents the product of the amount of DNA in the tail (expressed as a percentage of the total DNA) and the distance between the centers of mass of the head and tail regions as the measure of DNA damage. The comet tail moment was determined and the mean ± SD of the tail moment were obtained from 100 cells from each treatment group.

Densitometry

ImageJ software (National Institutes of Health) was used to quantify the mRNA and protein band intensities. Data are represented as relative to the intensity of the indicated loading control.

Statistical Analysis

Statistical comparisons were performed using (ANOVA) for analysis of significance between different values using GraphPad Prism software (San Diego, CA). Values are expressed as mean ± SE from at least three separate experiments, and differences were considered significant at a P value of less than 0.05.

Results

Changes in the Expression of DNA Damage Inducing and p53 Signaling-Mediated Apoptotic Genes After Spinal Cord Injury

To evaluate the changes in the expression of genes belonging to the DNA damage inducing and p53 signaling pathways involved after injury of rat spinal cord tissues, we performed cDNA microarray analysis using the RT2 profiler PCR array. We analyzed 84 genes each belonging to the above-mentioned two signaling pathways. Of the 84 apoptotic genes analyzed using p53 signaling RT-PCR microarray, 6 genes showed significant changes in samples taken 21 days after SCI (Table 1). Most of the pro-apoptotic genes were expressed at higher levels. Many genes related to p53 signaling, such as TP53, Cdc2 and Bag1 were upregulated after SCI (Table 1). Of the 84 DNA damage-inducing genes, 13 genes showed significant changes (Table 2). We observed the upregulation of DNA damage-inducing genes ATM, ATRx, Chek1, Ogg1, Gadd45a, TP53, Xrcc1 and PARP-I 21 days after SCI. Along with these genes, several genes of DNA repair enzymes were also detected. 60S ribosomal protein P1 and RAD21 homologue genes were downregulated. These results probably indicate that DNA damage response-mediated p53 signaling pathway genes may be causing the apoptosis observed during secondary pathogenesis of spinal cord injury. To assess DNA damage response-mediated apoptosis in injured spinal cord neuronal tissue,

Table 1 p53 signaling genes after spinal cord injury

Gene	Description	Fold up or down regulation
Bag1	Bcl2 associated gene	3.01
BRCA2	Breast cancer homolog2	2.06
Cdc2	Cell division cycle2 a	7.41
TP53	Tumor protein p53	3.61
Cip1/Waf1	Cyclin-dependent kinase inhibitor 1A	2.20
Ket/Tp63	Tumor protein p63	−4.47

Table 2 DNA damage inducing genes after spinal cord injury

Gene	Description	Fold up or down regulation
Apex	APEX nuclease (multifunctional DNA repair enzyme) 1	2.08
ATM	Ataxia telangiectasia mutated homolog (human)	7.93
Atrx	Alpha thalassemia/mental retardation syndrome X-linked (RAD54 homolog, *S. cerevisiae*)	5.74
Chek1	CHK1 checkpoint homolog (*S. pombe)*	3.15
Cspg6/bamacan	Structural maintenance of chromosomes 3	7.93
Gadd45a	Growth arrest and DNA-damage-inducible, alpha	5.35
TP53	Tumor protein p53	3.61
Xrcc1	X-ray repair complementing defective repair in Chinese hamster cells 1	4.661
Ogg1	8-oxoguanine DNA glycosylase	8.51
PARP1	Poly (ADP-ribose) polymerase 1	3.61
Tdg	Thymine-DNA glycosylase	14.79
RAD 21	RAD 21 homologue (*S. pombe*)	−5.84
Rlpl1	Ribosomal protein, large, P1	−2.49

we measured DNA fragmentation using the alkaline comet assay. This assay allows for the detection of both single-stranded and double-stranded DNA breaks and is therefore a highly sensitive method to directly examine the amount of DNA damage incurred in a single cell. Our results show that the extent of DNA damage increased from 1 day post-SCI to 21 days post-SCI (Fig. 1a), whereas there were no DNA strand breaks in the control spinal cord tissues. Since the number of DNA lesions in injured spinal cord tissues and upregulation of DNA damage-inducing molecules were observed by comet assay and DNA damage signaling RT-PCR array respectively, we decided to examine which proteins were playing a major role in DNA damage after SCI at different time points. We analyzed the tissue lysates using western blotting for the expression of ATM, ATR, CHK2, H2Ax, 8-OHdG, BRCA2 and Gadd45a (Fig. 1b). Expression of ATR and ATM increased with increased time periods. However, other molecules were highly expressed in the injured lysates compared to control with no significant changes over the time points (Fig. 1c). We further decided to confirm the DNA damage caused after SCI by carrying out immunohistochemical analysis of the spinal cord sections of the rats from sham control and those injured (21 days after SCI). We observed that immunoreactivity for 8-OHdG was null in sham control rats, and positive staining for 8-OHdG red fluorescence was more prominent in injured rats (21 days after SCI) (Fig. 1d). Furthermore co-localization experiments on spinal cord tissue sections adjacent to the site of injury with phosphorylated H2AX Ser^{139} and NF (neuronal filament) antibodies showed prominent expression of H2AX in the nucleus of neurons of the spinal cords of the injured group. Co-localization with neuronal factor staining confirmed the localization of H2AX activity in the nucleus of the neurons (Fig. 1e). Sham control spinal cord sections were negative for phospho-H2AX Ser^{139} fluorescence staining in the nucleus of neurons. These results suggest that DNA damage was induced in the neuronal population of injured rat spinal cords and activation of H2AX was observed in neurons of injured spinal cord sections.

Activated p53 Induces Apoptosis After SCI

Microarray analysis data demonstrated the upregulation of Bax and p53 genes after spinal cord injury. To further confirm the increase in p53 expression after spinal cord injury, we performed immunohistochemical analysis of the spinal cord sections of rats from sham control and injured (21 days SCI) groups by double immunostaining. Here, we specifically targeted the expression of p53 in three neural cell types (oligodendrocytes, astrocytes and neurons). p53 immunoreactivity was found primarily in glial cells where the nuclear localization of p53 is common. However, some glial cells also contained reaction product in their cytoplasm. p53-positive cells were co-localized to GFAP and Olig2, indicating that p53 is present in astrocytes and oligodendrocytes (Fig. 2a). In addition to these two cell types, we identified the expression of p53 in neurons (Fig. 2a). p53 was not detectable in sham operated control spinal cord tissue sections. Next, we estimated protein expression levels by western blotting. Total p53, phospho-p53 Ser^{392} and Bax levels were increased after 1 day and up to 21 days in injured spinal cords. On the other hand, levels of Bcl2, which is an anti-apoptotic protein, were drastically decreased by increased time points after injury (Fig. 2b, c). Finally, we performed p53 transcription factor assay using the Trans AM p53 transcription assay kit. Increased p53 transcription factor activity was observed in the nuclear

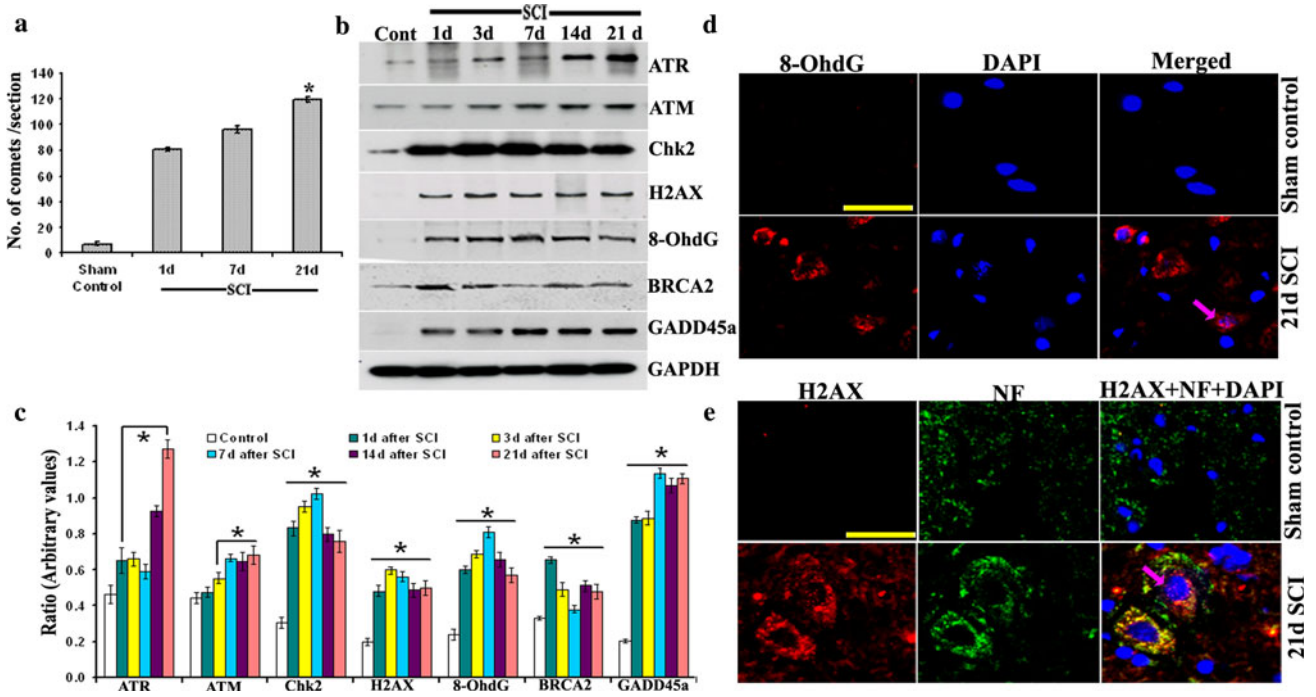

Fig. 1 DNA damage response after spinal cord injury. **a** Comet assay shows accumulation of DNA-SSBs and DNA-DSBs in injured rat spinal cords. Quantitation of damaged DNA in spinal neuronal cells was measured by the comet assay image analysis. *Columns* averages of three independent experiments with 100 cells (nuclei) analyzed per experiment. Values are mean ± SE based on at least 10 images per group and were replicated in 3 different rats spinal cords and comet assays. *Error bars* indicate mean ± SE. Significant at $P < 0.05$ vs. control cells. **b** DNA damage response elements were detected by Western blot analysis. Immunoblotting was done using antibodies against ATR, ATM, CHK2, H2AX, 8-OHdG, BRCA2 and Gadd45a. GAPDH was used as a control. Sham control, 1, 3, 7, 14 and 21 days post-SCI spinal cord tissue lysates were used for immunoblotting. **c** Quantitation of **b**. *Error bars* indicate mean ± SE. Significant at $P < 0.05$. **d** Immunohistochemical comparison of control, injured (21 days after SCI) spinal cord sections were performed to analyze the expression of 8-OHdG and **e** H2AX and NF colocalization at the site of injury. 8-OHdG is conjugated with Alexa Fluor 594 secondary antibody. H2AX is conjugated with Alexa Fluor 594 secondary antibody and NF is conjugated with Alexa Fluor 488 secondary antibody (n = 3). *Bar* = 200 μm

extracts of injured spinal cord tissues of 1, 7, 14 and 21 days post-SCI (Fig. 2d). Since p53 is involved in apoptosis, we evaluated the process of apoptosis in SCI tissues. Figure 3a shows the co-localization of p53-positive and TUNEL-positive cells in injured spinal cord (21 days SCI) but there were no TUNEL-positive or p53-positive cells detected in sham control sections. DNA laddering assay confirmed DNA fragmentation following the injury of spinal cords (Fig. 3b). These results confirm that p53 plays a role in induction of apoptosis after SCI.

Apoptosis is Mediated by the Mitochondrial Pathway

Accumulation of DNA damage leads to p53 activation through phosphorylation and subsequent apoptosis in cycling cells [19]. p53-mediated Bax activation and induction of caspase execution has been identified in several neurodegenerative diseases [5, 20]. p53 can mediate mitochondrial permeabilization through direct physical interaction with Bax and Bak. To confirm Bax-mediated apoptosis through the mitochondrial pathway, we prepared sub-cellular fractions from the mitochondrial and cytosolic fractions of sham control and injured spinal cords (3 weeks SCI). We carried out immunoblot analysis using Bax and cytochrome c antibodies. We observed increased Bax expression and decreased cytochrome c in the mitochondrial fractions of injured spinal cord tissue lysates. To check the purity of mitochondrial fractions, we analyzed the lysates with anti-HSP60 antibody (Fig. 3c, d). The mechanism by which p53 influences the neuronal response to injury is poorly understood. However, currently available data suggest that Bax mitochondrial translocation is involved in p53-mediated neuronal cell death [21, 22]. To confirm Bax activation in mitochondrial-mediated apoptosis, we performed Bax and HSP60 double immunohistochemical staining. Injured spinal cord tissue sections showed prominent expression of Bax co-localized with HSP60 in the neuronal population of injured tissue sections (Fig. 3e) while HSP60 and Bax co-localization was not detected in sham controls. Furthermore, activated expression of either p53 or Bax was not detected in sham controls. These results confirm the role of activated p53 in Bax

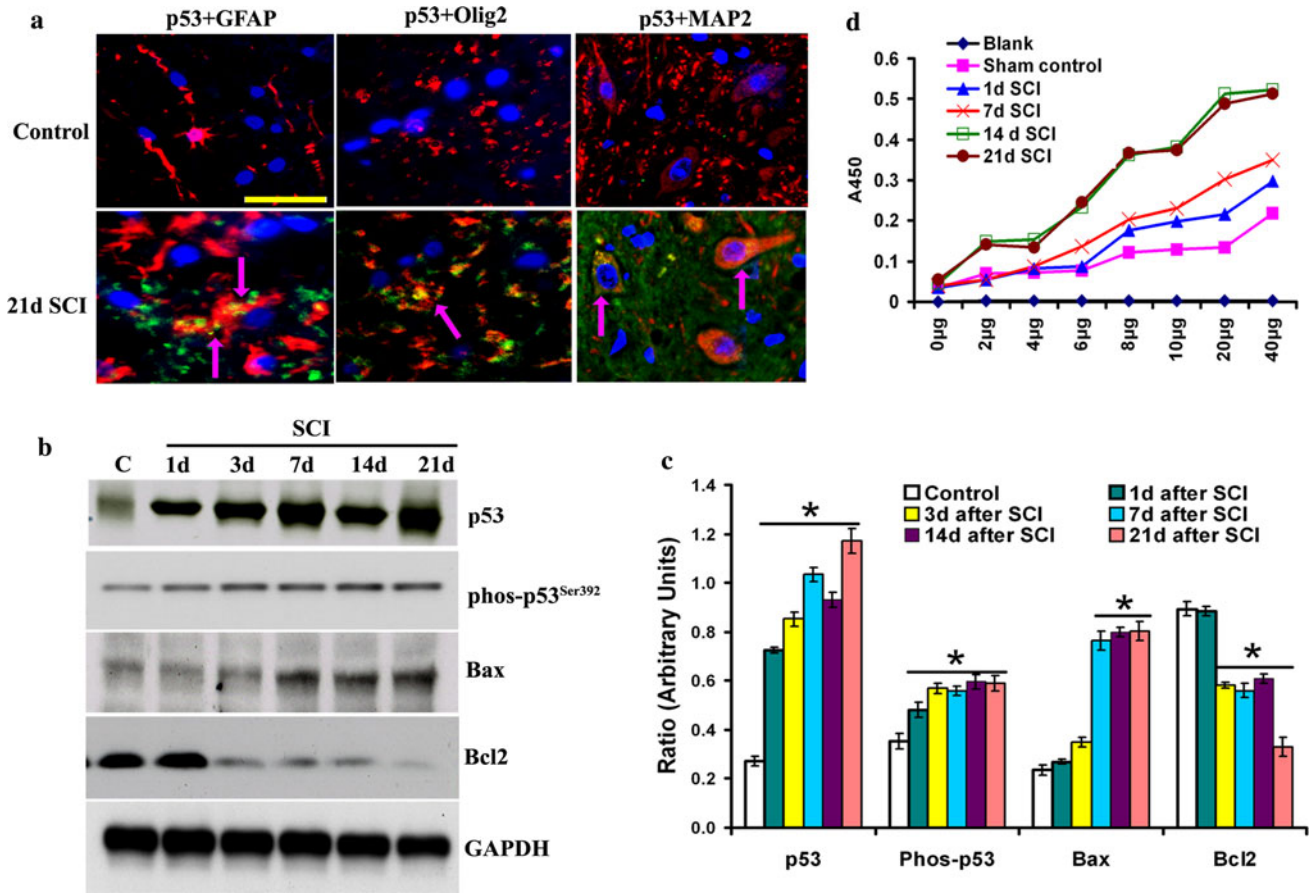

Fig. 2 Induction of apoptosis by activated p53 and Bax upregulation. **a** Immunohistochemical analysis of p53 in astrocytes, oligodendrocytes and neurons of injured spinal cord tissues (21 days post-SCI). GFAP (marker for astrocytes), Oligo2 (oligodendrocytes marker) and MAP2 (neuronal marker) were used. GFAP, Olig2 and MAP2 are conjugated with Alexa Fluor 594 secondary antibody and p53 is conjugated with Alexa Fluor 488 secondary antibodies. *Bar* = 200 μm. **b** Equal amounts of protein (40 μg) from sham controls and different time points of post-SCI samples were loaded onto 10–14% gels and transferred onto nitrocellulose membranes, which were then probed with their respective antibodies. GAPDH was used as a positive loading control. **c** Quantitation of **b**. *Error bars* indicate mean ± SE. Significant at $P < 0.05$. (D) p53 transcription factor assay. Sham control, 1, 7, 14 and 21 days post-SCI spinal cord tissues were used for nuclear extracts. We checked for p53 transcription factor activity using oligonucleotides that contained the p53 consensus DNA binding site (5′-GGACATGCCCGGG-CATGTCC-3′)

translocation and induction of apoptosis via the mitochondrial pathway. We next analyzed mitochondrial-mediated apoptotic pathway proteins using Western blot analysis. Immunoblotting showed that APAF1, cleaved caspase 9, cleaved caspase 3 and cleaved PARP-I protein expression were increased in all injured spinal cord tissue lysates from 3 to 21 days post-SCI. However, none of the above-mentioned cleaved fragments were detected in sham controls (Fig. 4a, b). Cytosolic cytochrome c induces the activation of APAF1, and it activates caspase 9 to form the APAF1-proteosome complex. The active proteosome complex further acts upon pro-caspase 3 and cleaves into an active form of caspase 3. Hence we measured the activation of caspase 9 and 3 by colorimetric estimation. We detected caspase 9 (Fig. 4c) and caspase 3 activity (Fig. 4d) in all injured tissue lysates (1, 3, 7, 14 and 21 days post-SCI). These results confirm the role of caspases 9 and 3 in p53-mediated neuronal cell death in injured spinal cord.

Activation of p53 in Staurosporine-Treated Spinal Neurons

Apoptosis and free radical damage are the prominent processes involved in secondary degeneration after spinal cord injury [23, 24]. Our in vivo experiments showed the activation of p53 in neurons after spinal cord injury. To assess the p53 activity due to apoptosis during secondary degeneration, we used an apoptosis-inducing agent, staurosporine (STP), to treat rat spinal neurons. Results of western blotting revealed the activation of p53 and Bax in STP-treated spinal neurons (Supplementary Figs. 1A, 1B). p53 and phospho-p53 Ser^{392} were significantly higher in STP-treated spinal neurons than in untreated cells.

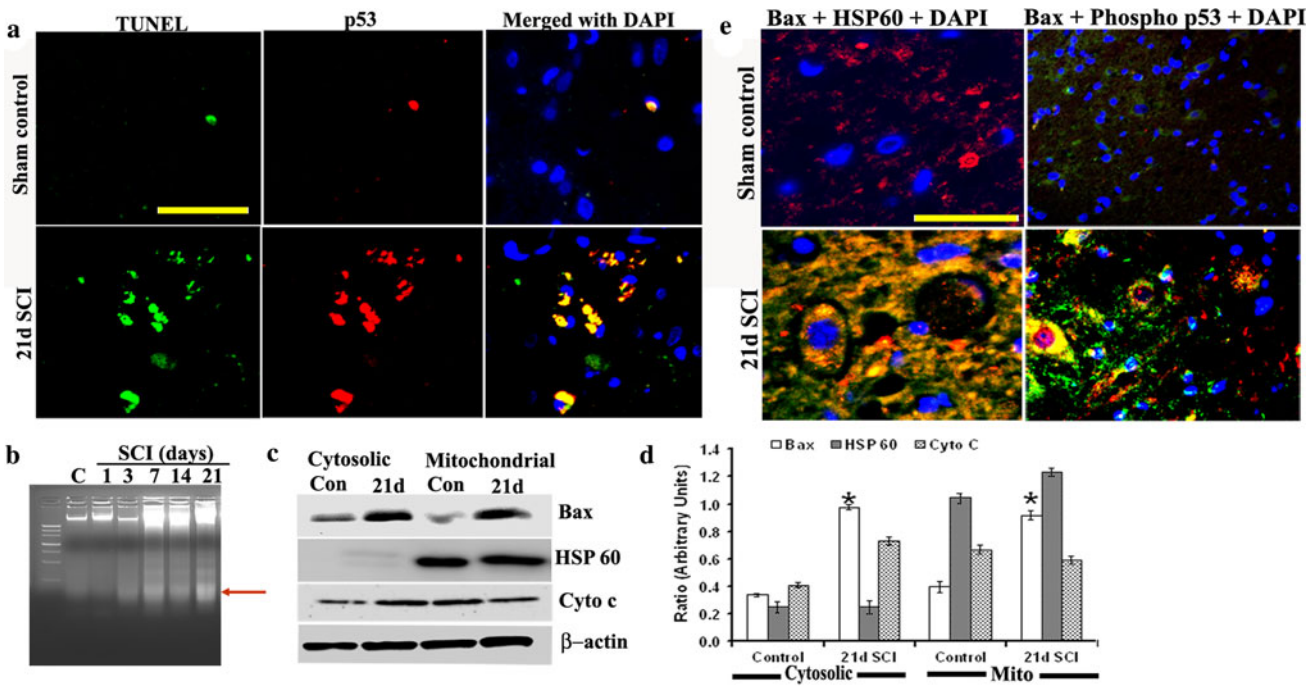

Fig. 3 Post-traumatic apoptosis after spinal cord injury in vivo. **a** Double labeling with terminal deoxynucleotidyl transferase dUTP nick end labeling (TUNEL) and co-localization with p53 staining by fluorescent-tagged secondary antibodies. TUNEL-positive and p53-positive cells were observed in injured spinal cord sections. *Bar* = 200 μm. p53 is conjugated with Alexa Fluor 594 secondary antibody. **b** DNA laddering analysis of sham control, 1, 3, 7, 14 and 21 days after spinal cord injury tissue sections. ~ 180 bp length DNA fragments were detected in injured tissue samples (←). **c** Mitochondrial and cytosolic fractions were analyzed for Bax and cytochrome c levels by western blotting. *β*-actin and HSP-60 were used as an internal control for the cytosolic and mitochondrial fractions, respectively. **d** Quantitation of **c**. *Error bars* indicate mean ± SE. Significant at $P < 0.05$. **e** Bax and HSP60 colocalization was analyzed by immunohistochemical staining of injured spinal cord tissues and compared with sham control sections. Bax is conjugated with Alexa Fluor 488 secondary antibody and HSP60 and phospho-p53 were conjugated with Alexa Fluor 594 secondary antibodies. Co-localization of phospho-p53 and Bax was detected in injured spinal cord tissues whereas no phospho-p53 and Bax staining was observed in the sham controls. All experiments were performed in triplicate. *Bar* = 200 μm

Immunocytochemical staining of p53 and phospho-p53 was observed in STP-treated spinal neurons (Supplementary Figs. 1C-D). We did not observe any expression of phospho-p53 Ser^{392} in control spinal neurons. Further, to confirm the in vivo experiments representing p53 activation and Bax-mediated apoptosis in injured spinal cords, we performed immunocytochemical analysis of spinal neurons that were injured with STP treatment. The amounts of red fluorescence, which is indicative of p53, and green fluorescence, which is indicative of Bax expression, were very slight in controls; expression increased when the cells were treated with STP (Supplementary Fig. 2A). In the merged images, p53 and Bax co-localization are clearly observable in STP-treated spinal neurons. Further, to confirm the activation and translocation of Bax into the mitochondria in injured spinal neurons, immunocytochemical analysis was performed on spinal neurons injured with STP. Spinal neurons were immunolabeled with anti-HSP60 and anti-Bax antibodies. As expected, we observed prominent yellow color, which is indicative of co-localization of HSP-60 and Bax expression, in injured spinal neurons. In contrast, we did not observe any expression of Bax or its localization with HSP-60 in control spinal neurons (Supplementary Fig. 2B). These results are consistent with our in vivo data and further strengthen the findings observed in vivo.

Discussion

The most important consequence of SCI is severe nerve injury that results from two mechanisms, primary trauma and secondary damage. The primary trauma induces mechanical compression, bleeding and electrolyte disturbances, which can lead to irreversible nerve injury. The secondary damage is due to edema, hemorrhage, inflammatory reaction, lipid peroxidative reaction, energy metabolism system disorders, ischemia and oxidative stress, which can give rise to reversible nerve injury. We hypothesized that after SCI, neuronal apoptosis is mediated by p53 involving the mitochondria. To validate our hypothesis, we analyzed the expression profiles of

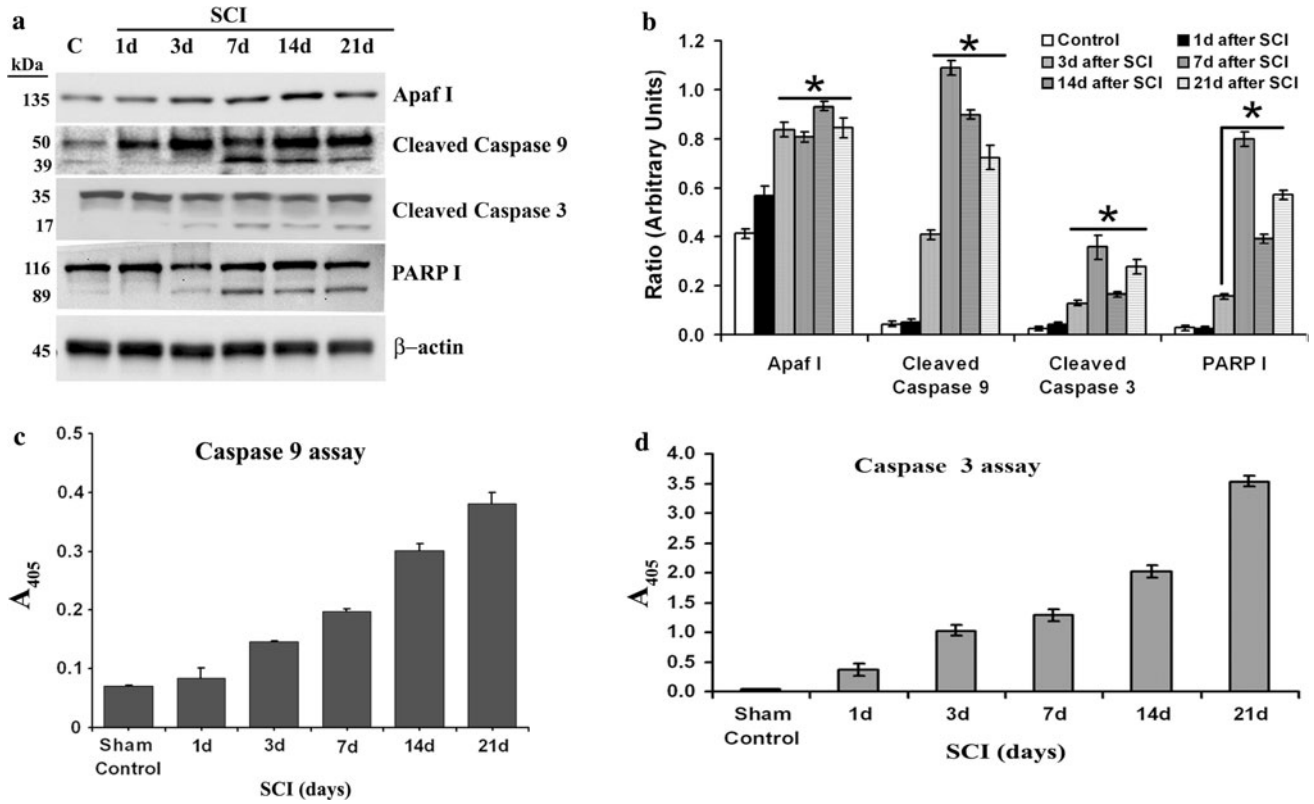

Fig. 4 Mitochondrial-mediated apoptotic pathway in spinal cord sections. **a** Equal amounts of protein (40 μg) were loaded onto 8–14% gels and transferred onto nitrocellulose membranes, which were then probed with respective antibodies. Beta-actin was used as a control. **b** Quantitation of **a**. *Error bars* indicate mean ± SE. Significant at $P < 0.05$. **c**, **d** Caspase 9 and caspase 3 activity in injured spinal cords. *Error bars* indicate SEM significant at $P < 0.005$. The experiment was repeated twice in triplicate (n = 3)

apoptotic genes 21 days after SCI and found efficient upregulation of apoptotic genes in the injured spinal cord. Thus, the results of this study demonstrate secondary degeneration after spinal cord injury caused by neuronal cell death. In this study, we attempted to characterize changes in gene expression levels in adult rats at 3 weeks post-SCI.

Details of the underlying mechanisms of DNA damage in the neuronal population of injured spinal cord tissues remain unknown. The present study is important because it strongly implicates the accumulation of DNA strand breaks as a major triggering event for neuronal apoptosis. Here, we also delineated the molecular mechanisms of DNA damage-induced apoptosis upstream and downstream of p53 in injured spinal cords. Our results show an increase in oxidative DNA damage scores (comet assay) in the nucleus of neuronal cells after spinal cord injury in the caudal section. However, DNA damage in other cell groups including glia, infiltrating leukocytes and endothelial cells of vascular walls might also be contributing to these changes [25]. In addition to direct DNA damage, DNA repair mechanisms can also be impaired after SCI. In this study, our immunohistochemistry results demonstrate increased expression of 8-OHdG and H2AX in injured spinal cords of the caudal region. Furthermore, RT-PCR microarray analysis showed that expression of DNA damage inducing genes were markedly increased after DNA damage post-SCI. These data suggest that 8-OHdG generation is one of the important mechanisms during inflammatory and secondary degeneration of spinal cord injury. The rapid accumulation of DNA strand breaks in the neuronal population of injured spinal cord tissues places DNA damage as an activator of the ATM/p53 regulated apoptosis cascade. Immunoblotting analysis showed increased expression of ATM and ATR, which are DNA-damage sensor kinases that become activated after increasing time points of injured spinal cords and in response to DNA damage; p53 and H2AX have been identified as active substrates in injured tissues.

Studies in transformed cell lines have led to a proposal that normal p53 degradation requires an intact nucleolus and that, in most cases, pro-apoptotic activation of the p53 signaling pathway is caused by nucleolar stress [26, 27]. Also, p53 dependent apoptosis and/or p53 activation were documented in neurons whose nucleoli were obliterated with camptothecin, or the transcriptional inhibitor

actinomycin D, or the knockdown/knockout of the Pol1 co-activator transcription initiation factor-1A [28, 29]. Cell cycle check point kinases Chk1 and Chk2 expression levels were increased and another DNA damage recognition marker protein, BCRA2, was elevated after spinal cord injury. The ATM kinase can mediate neuronal cell death in response to genotoxic stress through phosphorylation of p53 on serine-15 and serine-20 [30]. In addition, ATM-dependent pathways can indirectly contribute to p53 function by activating cyclin-dependent kinases and phosphorylation of MDM-2. In addition to the ATM/Chk2 pathway, other signalling cascades that mediate activation of p53 after DNA damage have been identified [30]. It is well established that p53 promotes apoptosis through enhanced transcription of specific target genes. [31, 32]. In p53-dependent neuronal apoptosis, the multi-domain Bcl-2 family member Bax has been identified as a major mediator of cell death [20, 33]. p53 is known to play a key role in determining cell death [34–37]. It is known that p53 induces death in tumor cells, which have abnormal DNA arrangements [38], and in cells exposed to DNA damaging agents [34]. Thus, at present, the role of p53 is considered to be dual; one is protective of the cell while the other induces apoptosis [39]. CNS injury is known to induce profound glial responses, including activation and proliferation. Yet, it is unclear what role might be served by p53 in the event of spinal cord injury in terms of cell protection or death.

Bcl2, an anti-apoptotic protein [40], is known to suppress Bax-induced apoptosis [41, 42] by forming a homodimer and a heterodimer [43]. In the present study, Western blot analyses showed increased phospho-p53 Ser^{392} and Bax expression in injured spinal cord tissues. Immunohistochemical analysis of injured tissue sections showed more staining for Bax and activated p53 than in the sham control tissues. Bax immunoreactivity was mainly co-localized with p53, suggesting that the cells were destined for apoptosis. These results confirm that p53-mediated Bax activation and translocation into the mitochondria further cause cytochrome c release into the cytosol. Activation of apoptosome by cytochrome c causes activation of caspase 3 and final PARP-I cleavage, which leads to DNA fragmentation in neuronal cells of injured spinal cord tissues. Furthermore, DNA laddering and TUNEL assays confirmed DNA fragmentation and p53-positive and TUNEL-positive cells in the neuronal population of the epicentre of injured spinal cord tissues. Immunohistochemical analysis of p53 in injured spinal cord tissues revealed the presence of p53 in all neuronal cells including neurons. In vitro experiments with STP-treated spinal neurons also confirmed our in vivo results. Mitochondrial translocation of Bax and p53 localization was observed both in vitro and in vivo. Taken together, the results of the present study identified apoptotic-signaling mechanisms at different time points after SCI, which may lead to future studies to establish protocols that can be used to ameliorate secondary injury mechanisms.

Acknowledgments We are thankful to Noorjehan Ali for technical assistance. We thank Shellee Abraham for manuscript preparation, and Sushma Jasti and Diana Meister for review of the manuscript. This study was funded by a grant from Caterpillar Inc., Peoria, IL and OSF Saint Francis Inc., Peoria, IL (J.S.R.).

References

1. Hong LZ, Zhao XY, Zhang HL (2010) p53-mediated neuronal cell death in ischemic brain injury. Neurosci Bull 26:232–240
2. Love S (2003) Apoptosis and brain ischaemia. Prog Neuropsychopharmacol Biol Psychiatry 27:267–282
3. Dasari VR, Veeravalli KK, Tsung AJ et al (2009) Neuronal apoptosis is inhibited by cord blood stem cells after spinal cord injury. J Neurotrauma 26:2057–2069
4. McEwen ML, Springer JE (2005) A mapping study of caspase-3 activation following acute spinal cord contusion in rats. J Histochem Cytochem 53:809–819
5. Morrison RS, Kinoshita Y, Johnson MD et al (2003) p53-dependent cell death signaling in neurons. Neurochem Res 28:15–27
6. Vekrellis K, McCarthy MJ, Watson A et al (1997) Bax promotes neuronal cell death and is downregulated during the development of the nervous system. Development 124:1239–1249
7. Morrison RS, Kinoshita Y (2000) The role of p53 in neuronal cell death. Cell Death Differ 7:868–879
8. Eve DJ, Dennis JS, Citron BA (2007) Transcription factor p53 in degenerating spinal cords. Brain Res 1150:174–181
9. Thornborrow EC, Patel S, Mastropietro AE et al (2002) A conserved intronic response element mediates direct p53-dependent transcriptional activation of both the human and murine bax genes. Oncogene 21:990–999
10. Gross A, Jockel J, Wei MC et al (1998) Enforced dimerization of BAX results in its translocation, mitochondrial dysfunction and apoptosis. EMBO J 17:3878–3885
11. Hsu YT, Youle RJ (1997) Nonionic detergents induce dimerization among members of the Bcl-2 family. J Biol Chem 272:13829–13834
12. Wolter KG, Hsu YT, Smith CL et al (1997) Movement of Bax from the cytosol to mitochondria during apoptosis. J Cell Biol 139:1281–1292
13. Desagher S, Osen-Sand A, Nichols A et al (1999) Bid-induced conformational change of Bax is responsible for mitochondrial cytochrome c release during apoptosis. J Cell Biol 144:891–901
14. Nomura M, Shimizu S, Ito T et al (1999) Apoptotic cytosol facilitates Bax translocation to mitochondria that involves cytosolic factor regulated by Bcl-2. Cancer Res 59:5542–5548
15. Brewer GJ, Price PJ (1996) Viable cultured neurons in ambient carbon dioxide and hibernation storage for a month. Neuroreport 7:1509–1512
16. Lee SM, Yune TY, Kim SJ et al (2003) Minocycline reduces cell death and improves functional recovery after traumatic spinal cord injury in the rat. J Neurotrauma 20:1017–1027
17. Liu XZ, Xu XM, Hu R et al (1997) Neuronal and glial apoptosis after traumatic spinal cord injury. J Neurosci 17:5395–5406
18. Dasari VR, Veeravalli KK, Saving KL et al (2008) Neuroprotection by cord blood stem cells against glutamate-induced apoptosis is mediated by Akt pathway. Neurobiol Dis 32:486–498

19. Giaccia AJ, Kastan MB (1998) The complexity of p53 modulation: emerging patterns from divergent signals. Genes Dev 12: 2973–2983
20. Xiang H, Kinoshita Y, Knudson CM et al (1998) Bax involvement in p53-mediated neuronal cell death. J Neurosci 18: 1363–1373
21. Chong MJ, Murray MR, Gosink EC et al (2000) Atm and Bax cooperate in ionizing radiation-induced apoptosis in the central nervous system. Proc Natl Acad Sci USA 97:889–894
22. Johnson MD, Xiang H, London S et al (1998) Evidence for involvement of Bax and p53, but not caspases, in radiation-induced cell death of cultured postnatal hippocampal neurons. J Neurosci Res 54:721–733
23. Amar AP, Levy ML (1999) Pathogenesis and pharmacological strategies for mitigating secondary damage in acute spinal cord injury. Neurosurgery 44:1027–1039
24. Crowe MJ, Bresnahan JC, Shuman SL et al (1997) Apoptosis and delayed degeneration after spinal cord injury in rats and monkeys. Nat Med 3:73–76
25. Schwab JM, Conrad S, Monnier PP et al (2005) Spinal cord injury-induced lesional expression of the repulsive guidance molecule (RGM). Eur J Neurosci 21:1569–1576
26. Olson MO (2004) Sensing cellular stress: another new function for the nucleolus? Sci STKE 2004:e10
27. Rubbi CP, Milner J (2003) Disruption of the nucleolus mediates stabilization of p53 in response to DNA damage and other stresses. EMBO J 22:6068–6077
28. Kalita K, Makonchuk D, Gomes C et al (2008) Inhibition of nucleolar transcription as a trigger for neuronal apoptosis. J Neurochem 105:2286–2299
29. Parlato R, Kreiner G, Erdmann G et al (2008) Activation of an endogenous suicide response after perturbation of rRNA synthesis leads to neurodegeneration in mice. J Neurosci 28:12759–12764
30. Keramaris E, Hirao A, Slack RS et al (2003) Ataxia telangiectasia-mutated protein can regulate p53 and neuronal death independent of Chk2 in response to DNA damage. J Biol Chem 278:37782–37789
31. Fridman JS, Lowe SW (2003) Control of apoptosis by p53. Oncogene 22:9030–9040
32. Slee EA, O'Connor DJ, Lu X (2004) To die or not to die: how does p53 decide? Oncogene 23:2809–2818
33. Cregan SP, MacLaurin JG, Craig CG et al (1999) Bax-dependent caspase-3 activation is a key determinant in p53-induced apoptosis in neurons. J Neurosci 19:7860–7869
34. Lowe SW, Ruley HE (1993) Stabilization of the p53 tumor suppressor is induced by adenovirus 5 E1A and accompanies apoptosis. Genes Dev 7:535–545
35. Manev H, Kharlamov A, Armstrong DM (1994) Photochemical brain injury in rats triggers DNA fragmentation, p53 and HSP72. Neuroreport 5:2661–2664
36. Shaw P, Bovey R, Tardy S et al (1992) Induction of apoptosis by wild-type p53 in a human colon tumor-derived cell line. Proc Natl Acad Sci USA 89:4495–4499
37. Wyllie A (1997) Apoptosis. Clues in the p53 murder mystery. Nature 389:237–238
38. Sandig V, Brand K, Herwig S et al (1997) Adenovirally transferred p16INK4/CDKN2 and p53 genes cooperate to induce apoptotic tumor cell death. Nat Med 3:313–319
39. Ford JM, Hanawalt PC (1997) Role of DNA excision repair gene defects in the etiology of cancer. Curr Top Microbiol Immunol 221:47–70
40. Chen G, Branton PE, Shore GC (1995) Induction of p53-independent apoptosis by hygromycin B: suppression by Bcl-2 and adenovirus E1B 19-kDa protein. Exp Cell Res 221:55–59
41. Oltvai ZN, Milliman CL, Korsmeyer SJ (1993) Bcl-2 heterodimerizes in vivo with a conserved homolog, Bax, that accelerates programmed cell death. Cell 74:609–619
42. Vaux DL, Korsmeyer SJ (1999) Cell death in development. Cell 96:245–254
43. Kroemer G (1997) The proto-oncogene Bcl-2 and its role in regulating apoptosis. Nat Med 3:614–620